



Cite this: *Environ. Sci.: Water Res. Technol.*, 2018, 4, 67

## Methane-driven microbial fuel cells recover energy and mitigate dissolved methane emissions from anaerobic effluents†

Siming Chen  and Adam L. Smith \*

The effluents of mainstream anaerobic treatment processes such as anaerobic membrane bioreactors (AnMBRs) contain dissolved methane that represents a large fraction of the available energy (approximately 50% at 15 °C) and a significant greenhouse gas (GHG) emission if released to the atmosphere. Microbial fuel cells (MFCs), which rely on exoelectrogenic microorganisms to generate electricity from organic or inorganic matter, could be used to recover energy and prevent GHG emissions from dissolved methane. Two replicate air-cathode, single-chamber MFCs and one dual-chamber MFC were constructed and operated in continuous mode on a synthetic, methane-saturated medium at 20 °C and hydraulic retention times of 4, 8, and 16 h. Up to 85% dissolved methane removal was achieved, resulting in the generation of  $0.55 \pm 0.06$  V. *Geobacter*, a common exoelectrogen, and methanotrophs were identified in anode biofilm samples by Illumina sequencing targeting the 16S ribosomal RNA (rRNA) and 16 rRNA gene. Activity quantification of key microbial populations *via* reverse transcription-quantitative polymerase chain reaction (RT-qPCR) indicated that methane removal and voltage production results from a consortium of aerobic methanotrophs enriched in a cathode biofilm that produce intermediate metabolites (*e.g.*, formate and acetate) that serve as substrates for *Geobacter* in the anode biofilm.

Received 2nd August 2017,  
Accepted 6th October 2017

DOI: 10.1039/c7ew00293a

rsc.li/es-water

### Water impact

Microbial fuel cells (MFCs) were evaluated to recover energy and prevent greenhouse gas emissions from dissolved methane in anaerobic effluents. Two air-cathode MFCs were used to demonstrate up to 85% dissolved methane removal and a maximum coulombic efficiency of 18% at 16 h hydraulic retention time. Multiple lines of evidence indicated a methanotroph–exoelectrogen interaction enabling energy recovery from dissolved methane.

## 1. Introduction

Anaerobic membrane bioreactors (AnMBRs) are a promising low-strength wastewater treatment technology combining anaerobic biological treatment with membrane separation in a single unit process. Wastewater organics are effectively converted into methane-rich biogas in AnMBRs which can subsequently be converted to electricity and heat. Further, AnMBRs have low sludge production, limited energy requirement assuming membrane fouling control is done efficiently, and similar carbon removal to aerobic processes at a range of operating temperatures.<sup>1,2</sup> However, AnMBRs produce an effluent saturated or supersaturated with dissolved methane,<sup>3</sup> dramatically increasing greenhouse gas (GHG) emissions rel-

ative to aerobic treatment processes if this methane is released to the atmosphere.<sup>4</sup> For example, approximately 50% of total produced methane remained in the dissolved form at 15 °C when treating a synthetic wastewater representative of domestic wastewater,<sup>5</sup> and at temperatures <5 °C, essentially all produced methane was dissolved in the effluent.<sup>1</sup> Although wastewater treatment plants are not regulated on GHG emissions, preventing these emissions and ideally recovering the embedded energy is necessary before AnMBRs or other mainstream anaerobic treatment processes can be responsibly implemented at the full scale.

Several studies have reported on the recovery or removal of dissolved methane from anaerobic effluents with varying success.<sup>6–13</sup> Giménez *et al.*<sup>6</sup> applied biogas-assisted mixing to sparge anaerobic effluents to avoid supersaturation of methane. However, methane losses of 42.6% and 46.6% at 30 °C and 20 °C, respectively, were still observed as biogas-assisted mixing only created equilibrium between gaseous and dissolved forms of methane. Limiting supersaturation may

Civil & Environmental Engineering, Astani Department of Civil and Environmental Engineering, University of Southern California, 3620 South Vermont Avenue, Los Angeles, CA 90089, USA. E-mail: smithada@usc.edu; Tel: +1 213 740 0473

† Electronic supplementary information (ESI) available. See DOI: 10.1039/c7ew00293a

enhance energy recovery *via* gaseous methane production but is insufficient to mitigate GHG emissions. To achieve GHG emissions similar to that in aerobic treatment, approximately 90% or more of dissolved methane needs to be removed from the AnMBR effluent.<sup>4</sup> To achieve dissolved methane removal beyond limiting supersaturation, membrane contactors in sweep gas desorption or vacuum degassing mode have been proposed.<sup>8–13</sup> However, energy demands for these proposed processes remain high, often an order of magnitude greater than energy available in recovered gaseous methane.

Biological treatment is another strategy for dissolved methane management, with aerobic methanotrophy and anaerobic oxidation of methane (AOM) being the most prevalent microbial pathways. AOM coupled with sulfate reduction or denitrification, referred to as denitrifying anaerobic methane oxidation (DAMO), has been reported extensively.<sup>14–18</sup> In DAMO, dissolved methane serves as the electron donor for denitrification *via* reduction of nitrate or nitrite and could thus potentially be used in a downstream nitrogen removal process.<sup>16,17</sup> It is important to note that AnMBRs and other mainstream anaerobic processes do not provide direct nutrient removal. Downstream DAMO processes would first require nitrification or nitrification of effluent ammonia which could be challenging without stripping dissolved methane into the gas phase or oxidizing it *via* aerobic methanotrophs, which may have higher oxygen affinity than DAMO microorganisms.<sup>19</sup> Aerobic methanotrophy is a multi-step metabolic pathway requiring oxygen to initially oxidize methane to methanol mediated by soluble/particulate monooxygenase. Then, methanol is either oxidized to formaldehyde, formate, and carbon dioxide or absorbed in the form of formaldehyde for biosynthesis of cellular components.<sup>20–22</sup> Under low oxygen availability, aerobic methanotrophs have been reported to release intermediate metabolites such as methanol, formaldehyde, and formate rather than completely mineralizing methane to carbon dioxide.<sup>23–25</sup> Matsuura *et al.*<sup>7</sup> reported using aerobic methanotrophy to oxidize dissolved methane in down-flow hanging sponge reactors, similar to trickling filters. Although these systems efficiently prevent GHG emissions – removal efficiencies of 70% in a one-stage system and up to 99% in a two-stage system – they fail to recover energy and require energy input to supply oxygen. Potentially more promising, methanotrophs could be used to recover biomaterials such as polyhydroxyalkanoate (PHA),<sup>26</sup> but this line of research requires further investigation before it becomes a realistic strategy for dissolved methane management in anaerobic effluents. Despite the various physical and biological approaches evaluated to date for dissolved methane management, feasibility remains questionable and effluent dissolved methane persists as a barrier to mainstream anaerobic treatment.

Microbial fuel cells (MFCs), bioelectrochemical systems where microorganisms directly deposit electrons to an anode during oxidation of organic or inorganic compounds,<sup>27–29</sup> have traditionally been studied for energy recovery directly from domestic wastewater and thus can be seen as a direct

competitor to mainstream anaerobic treatment.<sup>28,30</sup> Single-chamber, air-cathode MFC designs allow for a system with essentially no energy demands due to oxygen being provided passively at the atmosphere-exposed cathode.<sup>27</sup> MFCs have been demonstrated with anaerobic post-treatment<sup>31–33</sup> as a coupled approach for domestic wastewater treatment. For example, Ren *et al.*<sup>31</sup> demonstrated an MFC coupled with an anaerobic fluidized bed membrane bioreactor and were able to produce a high-quality effluent with minimal energy requirements. However, in such configurations, residual chemical oxygen demand (COD) from the MFC does not provide sufficient organics for the anaerobic treatment system to produce gaseous methane and therefore recover energy. The anaerobic treatment system essentially acts to convert residual COD from the MFC into dissolved methane. We propose to invert this configuration and operate an MFC downstream of an anaerobic treatment system to recover energy and prevent GHG emissions from dissolved methane. This configuration eliminates any risk of dissolved methane being stripped and released from anaerobic effluents. Further, MFCs are an attached growth process and thus biological post-treatment of AnMBR effluents may be possible without subsequent removal of solids. A methane-driven MFC could also be used to power underwater sensors in marine applications<sup>34,35</sup> or to convert gaseous methane (*i.e.*, natural gas) into electricity to reduce or eliminate methane leaks that occur during transportation and storage.<sup>36</sup>

An early 1965 study by van Hees<sup>37</sup> reported using methane as the only organic in a two-chamber MFC that produced 0.5–0.6 V using a pure culture of *Pseudomonas methanica*. This work suggested that a methanotroph could act as an exoelectrogen similar to *Geobacter*, a common exoelectrogen in MFCs. However, no reports of exoelectrogenic methanotrophs exist outside of this study. It is important to note that *Geobacter* does not have the metabolic pathways for direct methane oxidation. A recent study reported a two-chamber MFC using methane as the electron donor at the anode inoculated with DAMO-archaea.<sup>38</sup> A relatively low voltage production was reported but there was a correlation between voltage and methane addition to the anode chamber. The anode was enriched with DAMO-archaea and *Geobacter*, suggesting that these populations may work together to deposit electrons on the anode. Recently, McAnulty *et al.*<sup>39</sup> demonstrated electricity production from methane in a two-chamber MFC by constructing an engineered archaeal strain capable of producing methyl-coenzyme M reductase to convert methane to acetate (*i.e.*, reverse methanogenesis). With the aid of electron shuttles and methane-acclimated sludge containing *Paracoccus denitrificans*, *Geobacter sulfurreducens* was shown to generate electricity from methane *via* this synthetic microbial consortium.

This study is the first to investigate the potential for air-cathode MFCs to be used as a post-treatment biotechnology for energy recovery and mitigation of GHG emissions from anaerobic effluents. The performance of bench-scale, methane-driven MFCs was evaluated using a synthetic

medium representative of an AnMBR effluent produced during domestic wastewater treatment. Process performance was evaluated at hydraulic retention times (HRTs) of 16, 8, and 4 h by measuring voltage production, dissolved methane removal efficiency, and other water quality parameters. High-throughput sequencing targeting 16S ribosomal RNA (rRNA) and 16 rRNA genes and reverse transcription-quantitative polymerase chain reaction (RT-qPCR) were used to evaluate the microbial community structure and activity of anode and cathode biofilms.

## 2. Materials and methods

### 2.1 MFC configurations

Two replicate single-chamber, air-cathode MFCs with a 240 mL working volume were constructed based on the design of those reported in ref. 40. Three carbon brushes (Zoltek PX 35 carbon fiber, Mill-Rose Company, Mentor, OH) with a 2.5 cm diameter and 5 cm length were used as the anode. Carbon nanofibers were twisted on a titanium rod which provided current collection. The anodes were pretreated by soaking the brushes in a solution of ammonium peroxydisulfate (200 g L<sup>-1</sup>) and concentrated sulfuric acid (100 mL L<sup>-1</sup>) for 15 min according to ref. 41. A carbon cloth (30% wet-proofing, carbon cloth CC4 wet proofed, Fuel Cell Earth, Woburn, MA) was pretreated as described in ref. 42 for use as the cathode. Two pieces of fabric cloth (Amplitude EcoCloth, Contect, Inc., Spartanburg, SC) were integrated between the anode and the cathode as a separator to prevent excess oxygen diffusion and potential short-circuiting. Reactors were operated with 1000 ohm resistance in the external circuit. A data acquisition device (DI245, DATAQ, Akron, OH) was used to measure voltage every 16 s and subsequent data were trimmed to every 20 min for analysis. Reactors were located in a temperature controlled incubator (*Drosophila* Incubator, Genesee Scientific, CA) and the synthetic wastewater medium (ESI† Table S1) was placed in a refrigerated water bath (Lindberg/Blue M Shaking Water Bath, Thermo Fisher Scientific, Waltham, MA) such that both maintained a temperature of 20 °C. Initially, both replicate MFCs were filled with a medium composed of half primary effluent (120 mL) from the Hyperion Wastewater Treatment Plant (Los Angeles, CA) and half synthetic medium (120 mL) consisting of acetate and nutrients to inoculate the MFCs. The inoculum was screened for the presence of *Geobacter* and methanotrophs *via* PCR and gel electrophoresis (methodology described below; ESI† Fig. S1). After demonstrating stable and reproducible voltage production, both MFCs were operated on acetate containing synthetic medium in batch mode to benchmark the performance of our system against similar systems fed acetate reported in the literature.

Next, the MFCs were operated in continuous mode on a synthetic anaerobic methane-saturated medium with dissolved methane as the only organic (no acetate was in the medium). Methane was dissolved in the medium by vigorously purging with an 80% methane and 20% carbon dioxide gas mixture for 15 min. The me-

dium was kept in gas-tight containers and constantly bubbled with the gas mixture at 10–20 mL min<sup>-1</sup> to ensure influent dissolved methane concentration and prevent intrusion of atmospheric oxygen. The system was initially operated at an 8 h HRT which was later varied to evaluate performance at 16, 8, and 4 h HRTs.

A two-chamber MFC was constructed using the same electrode materials as the single-chamber MFCs with glass reaction chambers (MFC 250.40.0, Adams & Chittenden Scientific Glass, Berkeley, CA). Inoculation and batch mode operation was performed similarly to the single-chamber MFCs. The anode chamber was continuously fed with methane containing medium, while the cathode chamber was continuously sparged with air. A cation exchange membrane (CMI-7000, Membranes International Inc., Ringwood, NJ) was placed between the anode and cathode chambers for proton exchange.

Power density,  $P_{\text{cat}}$ , defined as power generation normalized by the cathode area, was used to characterize MFC power production and compare with relevant MFCs reported in the literature:

$$P_{\text{cat}} = \frac{V^2/R}{A_{\text{cat}}}$$

where  $V$  is the voltage production,  $R$  is the resistance, and  $A_{\text{cat}}$  is the cathode area (60 cm<sup>2</sup>).

Coulombic efficiency (CE) defines the percentage of electrons recovered in the form of electricity over total electrons originating from available organics. Dissolved methane can thus be converted to theoretical maximum current (TMC) and converted to CE with the actual current (AC). TMC and CE were calculated as follows:

$$\text{TMC} = \frac{D_{\text{CH}_4} C b F Q}{M R}; \quad \text{CE} = \frac{\text{AC}}{\text{TMC}}$$

where  $D_{\text{CH}_4}$  is the dissolved methane concentration (mg L<sup>-1</sup>),  $C$  is the COD equivalent of methane (4 g O<sub>2</sub> per g CH<sub>4</sub>),  $b$  is the number of electrons transferred per mole of oxygen,  $F$  is Faraday's constant,  $Q$  is the incoming flow rate,  $M$  is the molecular weight of oxygen, and  $R$  is the resistance in the external circuit (1000 Ω).

### 2.2 Chemical assays

pH and dissolved oxygen (DO) were measured with a pH probe (SevenCompact pH/Ion S220, Mettler Toledo) and a DO meter (SevenGo Duo pro SG98, Mettler Toledo), respectively. Influent and effluent dissolved methane concentrations were measured daily and influent DO was measured periodically to confirm that the influent remained anaerobic. Dissolved methane in the synthetic medium and effluent was stripped out of the liquid by vigorously shaking for 1 min in a gas-tight syringe in the presence of an equal volume of nitrogen. Then, 1 mL of the resulting methane and nitrogen mixture was injected into a Trace 1310 gas chromatograph (Thermo

Fisher Scientific, Waltham, MA) equipped with a 30 m × 0.53 mm × 20 μm TracePLOT TG-BOND Q column and a flame ionization detector to quantify the methane content. The instrument was operated in split injection mode, with the inlet temperature at 250 °C, the oven at a constant 150 °C, and the detector at 250 °C. Dissolved methane concentration was then calculated based on the methane content using the ideal gas law:

$$c_{\text{CH}_4} \left( \text{mg L}^{-1} \right) = \frac{PV}{RT} \frac{M_{\text{CH}_4}}{V_1}$$

where  $V_1$  is the volume of influent or effluent sample,  $P$  is the atmospheric pressure (1 atm),  $V$  is the volume of methane stripped out of the liquid sample,  $R$  is the ideal gas constant,  $T$  is the operating temperature (20 °C), and  $M_{\text{CH}_4}$  is the molecular weight of methane.

Volatile fatty acids (acetate, formate, propionate, butyrate, and valerate) and inorganic ions (chloride, phosphate, sulfate, and nitrate) were quantified by ion chromatography (ICS 2100, Thermo Fisher Scientific, Waltham, MA) using a 2 mm AS-11HC column (Dionex, Sunnyvale, CA). Samples were filtered using 0.2 μm Whatman filters (GE Healthcare Life Sciences, Pittsburgh, PA) and loaded into a temperature controlled autosampler at 4 °C before being injected. The instrument was operated at an eluent flow rate of 0.5 mL min<sup>-1</sup> with an eluent KOH concentration of 1 mM during the first 15 min and then linearly ramped to 60 mM until the end of the run (total run time of 28 min). Standards containing VFAs and inorganic ions were prepared and run in triplicate at 1, 5, 10, and 50 mg L<sup>-1</sup>.

### 2.3 Microbial community structure and activity

Anode and cathode biomass samples were collected periodically from bench-scale MFCs and immediately stored at -80 °C. RNA samples were preserved in DNA/RNA Shield (Zymo Research, Irvine, CA). DNA was extracted from biomass by initially mixing with prebaked 0.1 mm diameter zirconium beads and lysis buffer, followed by three, 2 min bead beating steps (Mini-Beadbeater-24, BioSpec Products, Bartlesville, OK). The supernatant was taken and digested with proteinase K followed by automated extraction *via* a Maxwell® magnetic particle processor (Promega, Madison, WI) using Maxwell 16 LEV Blood DNA kits according to the manufacturer's instructions. RNA was extracted in three, 1 minute zirconium bead beating steps using lysis buffer and 1-thioglycerol from a Maxwell 16 LEV simplyRNA blood kit, followed by automatic extraction according to the manufacturer's instruction. DNA and RNA extracts were quantified by spectrophotometry (BioSpectrometer Fluorescence, Eppendorf, Germany). After that, the DNA concentration was further quantified *via* the Quant-iT™ PicoGreen dsDNA Assay (Thermo Fisher Scientific, Waltham, MA). RNA extracts went through an additional treatment to remove DNA contamination using the Invitrogen

DNA-free DNA removal kit (Thermo Fisher Scientific, Waltham, MA). PCR amplification of contaminating 16S rRNA genes and gel electrophoresis were performed to ensure RNA purity (ESI† Fig. S2). RNA was then quantified using a Quant-iT™ RiboGreen RNA assay kit (Thermo Fisher Scientific, Waltham, MA). After that, RNA samples were reverse transcribed to generate complementary single-stranded DNA (cDNA) using the GoScript reverse transcription system (Promega, Madison, WI).

Illumina MiSeq sequencing targeting the V4 region of bacteria and archaea was performed by the Host Microbiome Initiative (University of Michigan, Ann Arbor, MI). A set of barcoded primers described by Kozich *et al.*<sup>43</sup> were used to sequence 16S rRNA and 16S rRNA genes. PCR reactions were conducted using the following reagent composition: primers at 500 nM, 10 μL 2× Accuprime buffer 11 (Invitrogen, Waltham, MA), 0.15 μL Accuprime HiFi TAQ, 0.5 ng template, and nuclease-free water in a total volume of 20 μL. Thermocycling included an initial 2 min denaturation at 95 °C followed by 30 cycles of denaturing at 95 °C for 20 s, annealing at 55 °C for 15 s, and extension at 72 °C for 5 min, with a final extension at 72 °C for 5 min. SequalPrep Normalization Plate Kits (Life Technologies, Grand Island, NY) were used to pool amplicons by equal mass. Multiplexed amplicons were sequenced *via* Illumina MiSeq using a MiSeq reagent kit V2 (2 × 250 bp reads) at the University of Michigan. Mothur<sup>44</sup> was used to analyze sequencing results following the Schloss MiSeq SOP. The UCHIME algorithm was applied to perform chimera removal. After quality filtering, an average of 23 431 ± 3364 paired-end sequences per sample were obtained, with minimum and maximum sequences of 21 627 and 28 474. Sequences were aligned with the SILVA reference database<sup>45</sup> and were subsampled to 21 627 sequences before conducting further analysis with operational taxonomic unit (OTU)-based clustering (average neighbor algorithm at 3% cutoff) of subsampled sequences.

Primers for RT-qPCR were used to target *Geobacter* (Geo564F (AAGCGTTGTCGGAWTTAT) and Geo840R (GGCACTGCAGGGGTCAATA)),<sup>46</sup> particulate methane monooxygenase (*pmoA*; a functional gene of methanotrophs, A189F (GGNGACTGGGACTTCTGG) and mb661R (CCGGMGCAACGTCYTTACC)),<sup>47</sup> and the 16S rRNA V4 region of bacteria and archaea (515F (GTGCCAGCMGCCGCGGTAA) and 806R (GGACTACHVGGGTWTCTAAT))<sup>43</sup> in RNA extracts from cathode and anode biofilm biomass. RT-qPCR was conducted in 15 μL reactions on a LightCycler® 96 instrument (Roche Molecular Systems, Inc.) with 7.5 μL qPCR master mix (Fast Plus EvaGreen® qPCR master mix, Biotium), 0.3 μM for forward and reverse primers, 1 μL cDNA template, and DNase/RNase-free water. RT-qPCR standards were generated using the aforementioned primers in 10 μL reactions on a Mastercycler® Nexus thermocycler (Eppendorf, Germany) with 5 μL PCR master mix (NEBNext® Q5® Hot Start HiFi PCR Master Mix, New England BioLabs® Inc.), 1 μM forward and reverse primers, and 2 μL cDNA template pooled from reverse transcribed RNA extracts of samples from the bench-

scale MFCs. Isolated PCR products were run on an agarose gel, purified with the Wizard® SV Gel and PCR Clean-Up System (Promega, Madison, WI), and quantified with QuantiT™ PicoGreen (Thermo Fisher Scientific, Waltham, MA), after which serial dilutions of  $10^8$  to  $10^1$  copies of each gene were prepared. PCR and RT-qPCR temperature cycling programs are shown in the ESI† Table S2.

### 3. Results and discussion

#### 3.1 Preliminary findings suggest methane removal and voltage production driven by co-culture of methanotrophs and *Geobacter*

The replicate bench-scale MFCs (reactors A and B) were first fed a  $1000 \text{ mg L}^{-1}$  acetate-containing medium to enrich for exoelectrogens, particularly *Geobacter*, from the primary effluent inoculum. Stable and repeatable voltage production was observed during two batch runs (ESI† Fig. S3), suggesting

successful acclimation of *Geobacter* on the anode. The replicate MFCs were then switched to continuous operation with a saturated methane-containing medium (no acetate present). A voltage plateau of 0.5 to 0.6 V was recorded which is in agreement with results commonly obtained for similar MFCs operated on acetate or domestic wastewater.<sup>40,48</sup> During 50 days of operation, voltage production averaged  $0.476 \pm 0.122 \text{ V}$  and  $0.334 \pm 0.117 \text{ V}$  for reactors A and B, respectively (Fig. 1a). Dissolved methane removal efficiency averaged  $28.3 \pm 9.7\%$  and  $24.6 \pm 8.6\%$ , which resulted in a CE of  $4.53 \pm 1.23\%$  and  $2.85 \pm 0.17\%$  for reactors A and B, respectively (Fig. 1b). Low CE was attributed to low dissolved methane removal efficiency and relatively low voltage production coupled with a high dissolved methane loading.

The microbial community structure and activity data derived from high-throughput sequencing indicated a high activity of *Geobacter* and aerobic methanotrophs in the anode biofilm, suggesting that enrichment of these populations was

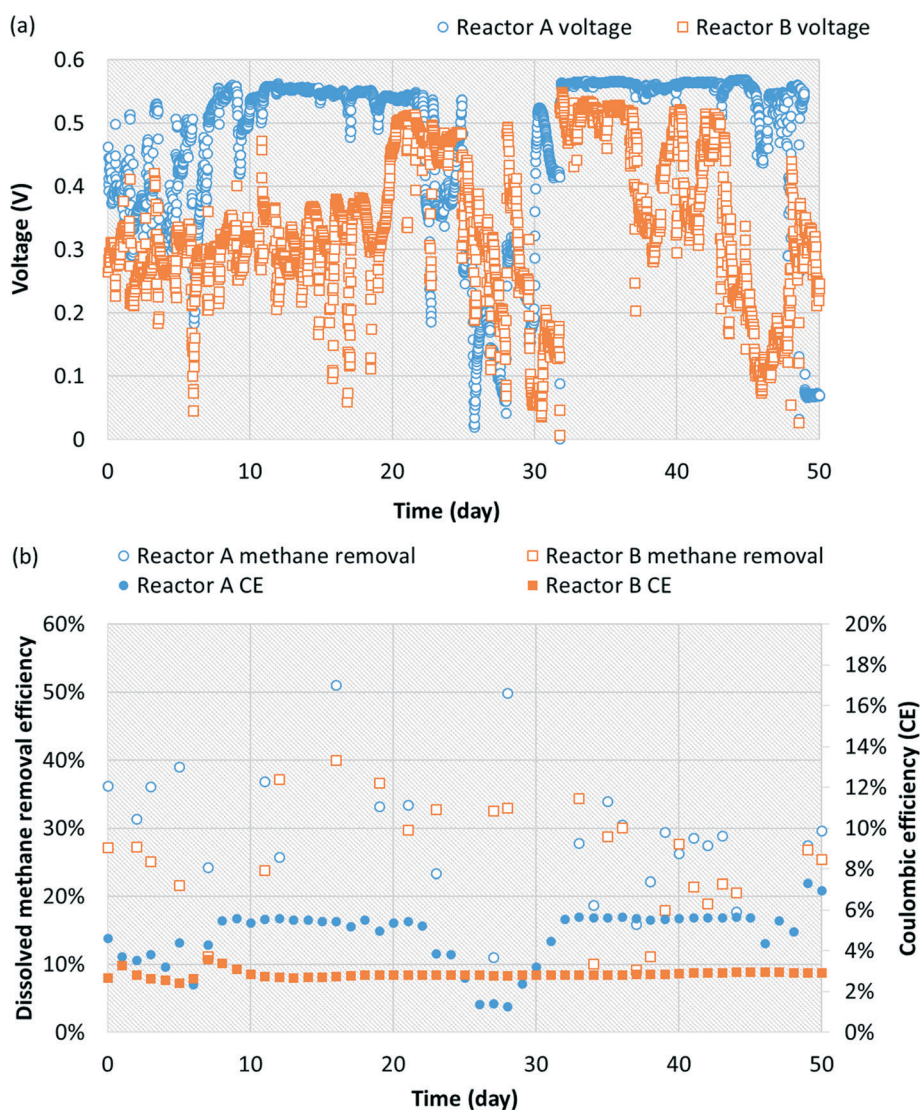


Fig. 1 (a) Voltage production and (b) dissolved methane removal efficiency and coulombic efficiency (%) over time from initial continuous operation of replicate air-cathode, single-chamber MFCs fed methane-saturated medium.

necessary to convert dissolved methane to electrons. The relative abundance of *Geobacter* at the anode was 23.1% and 20.9% in reactors A and B, respectively (Fig. 2). The relative activity of *Geobacter* was more variable at 41.9% and 6.31% in reactors A and B, respectively. The high variability in relative activity may have resulted in differences in performance immediately prior to sampling or our sampling protocols since RNA has a relatively short half-life. An OTU classifying within the family Bradyrhizobiaceae comprised 1.00% and 2.65% relative abundance and 1.51% and 7.28% relative activity in reactors A and B, respectively. A representative sequence from this OTU demonstrated high identity (94%) with *Rhodopseudomonas palustris*, a population isolated from an MFC capable of producing a higher power density than mixed microbial communities.<sup>49</sup> Aerobic methanotrophs in reactors A and B anode biofilms comprised 2.50% and 2.96% of relative abundance and 4.10% and 5.11% of relative activity, respectively. Aerobic methanotrophs classified as *Methylomonas methanica*, a species previously classified as *Pseudomonas methanica* and used extensively as a model methanotroph.<sup>50</sup> This same population was used in the pure culture methane-driven MFC reported previously.<sup>37</sup> These preliminary sequencing results suggest that oxygen diffusion through the cathode fueled initial methane oxidation to intermediate metabolites, likely formate, that could be converted to electrons by *Geobacter*. Thus far, there have been no reports of *Geobacter* directly metabolizing other potential intermediates in aerobic methanotrophy (*i.e.*, methanol or formaldehyde). However, it is also possible that acetogens converted intermediate metabolites of aerobic methanotrophy to acetate *via* acetogenesis. Therefore, *Geobacter* at the anode may have converted both formate and

acetate to electrons. Trace amounts of acetate in the reactor effluent were occasionally detected (data not shown), suggesting that acetogenesis from intermediate metabolites of aerobic methanotrophy did indeed occur. Despite the previous findings by van Hees,<sup>37</sup> it is unlikely that a methanotroph was acting as an exoelectrogen in our MFCs given the relatively low activity of methanotrophs at the anode and the high activity of *Geobacter*. A limitation of this preliminary sequencing work is that only the anode biofilm was sampled. A cathode biofilm was also likely present and may have contained significant activity of methanotrophs given that DO concentrations within the reactor are highest at the cathode due to diffusion from the atmosphere. In later work, both the anode and the cathode biofilms were characterized.

To evaluate the impact of DO on MFC performance in more controlled experimentation, we operated a two-chamber MFC with influent containing varying DO concentrations of 0, 0.5, 1, and 2 mg L<sup>-1</sup> by purging the influent medium with pure methane until the desired DO was achieved (ESI† Fig. S4). We observed a similar positive correlation between voltage production and influent DO concentration as was reported in a U.S. patent on methane powered MFCs<sup>35</sup> and a recent study on DAMO MFC.<sup>38</sup> Initially, voltage at 0 mg L<sup>-1</sup> and 0.5 mg L<sup>-1</sup> DO stabilized at around 0.0957 ± 0.0356 V and 0.0784 ± 0.0503 V over 20 days of operation. After that, the MFC was switched to 1 mg L<sup>-1</sup> DO medium for 2 days and 2 mg L<sup>-1</sup> DO medium for more than 1 week. The voltage increased to 0.272 ± 0.100 V and 0.370 ± 0.026 V with peak voltage surging to approximately 0.4 V. DO was then reduced to 0.5 mg L<sup>-1</sup> and the voltage decreased to 0.199 ± 0.067 V. The correlation between influent DO concentration and

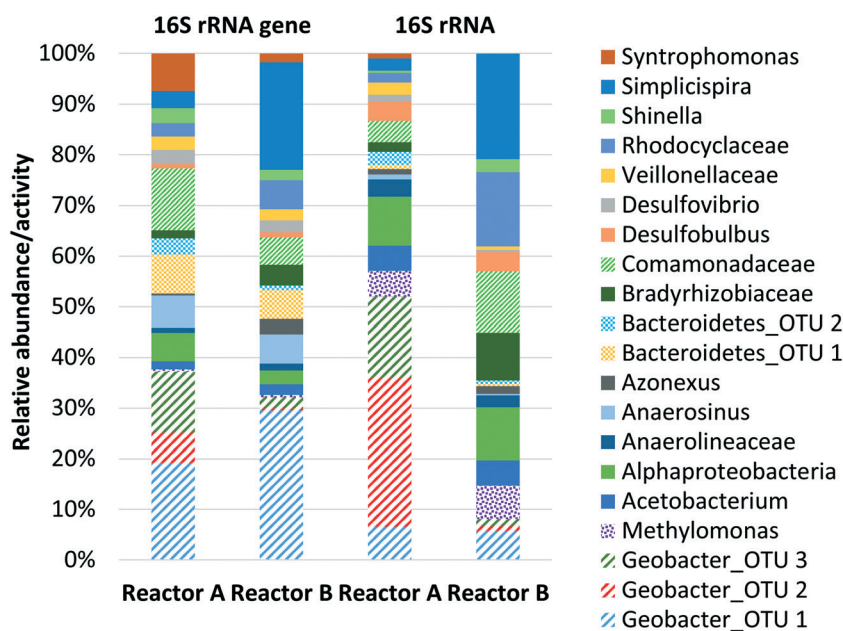


Fig. 2 Relative abundance and relative activity based on 16S rRNA gene and 16S rRNA sequencing, respectively, of reactors A and B anode biofilms identified to the genus level where possible. All data are expressed as a percentage normalized using total 16S rRNA gene and 16S rRNA sequences (bacteria and archaea).

voltage production confirmed our hypothesis that DO impacts aerobic methanotrophy and intermediate metabolite availability for exoelectrogens. This motivated further evaluation of HRT in the single-chamber MFCs, which directly controls oxygen availability from diffusion through the cathode.

### 3.2 Dissolved methane removal efficiency strongly correlated with HRT

Both replicate MFCs were operated at HRTs of 4, 8, and 16 h to evaluate a potential correlation with dissolved methane removal due to increased oxygen diffusion relative to dissolved methane loading at higher HRTs. Oxygen diffusion through the cathode is constant over time, and thus increasing HRT increases oxygen availability relative to influent methane loading. At an HRT of 16 h, reactors A and B produced  $0.61 \pm 0.01$  and  $0.51 \pm 0.06$  V, respectively (Fig. 3a). When both MFCs were reduced to an HRT of 8 h, reactor A voltage production remained almost the same at  $0.59 \pm 0.07$  V, whereas

reactor B voltage decreased to  $0.33 \pm 0.08$  V. At an HRT of 4 h, reactor A and B voltage production decreased significantly to  $0.11 \pm 0.04$  V and  $0.30 \pm 0.05$  V, respectively. Occasional performance irregularities occurred (e.g., voltage decrease or high variability), which were attributed to factors such as bio-fouling on the cathode, pump system malfunction, air intrusion into the anaerobic medium container during medium replacement, *etc.* One concern is that dissolved methane could be removed from the system *via* diffusion out of the reactor chamber through the separator and cathode. To evaluate this concern, a small chamber adjacent to the cathode was sealed from the outside environment to prevent gas exchange. Gaseous methane concentrations within this chamber were quantified for reactors A and B over time (4, 8, and 16 h after sealing the chamber). Gaseous methane concentrations in the chamber correlated linearly with time ( $R^2 = 0.944$ ) with a maximum concentration after 16 h representing 1.61% and 1.71% of the total methane loading for reactors A and B, respectively. This indicates that fugitive methane loss

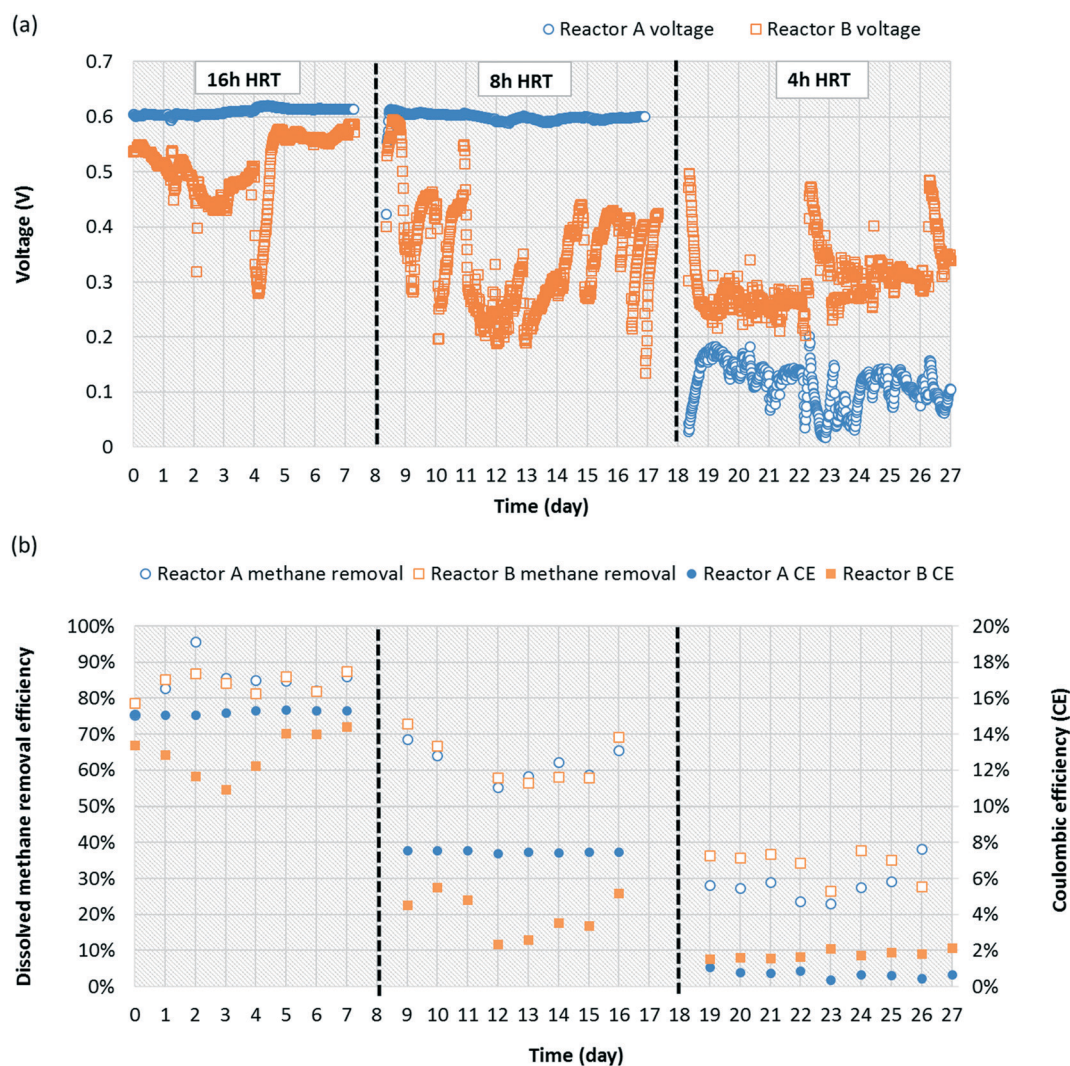


Fig. 3 (a) Voltage production and (b) dissolved methane removal efficiency and coulombic efficiency (%) over time for reactors A and B during continuous operation on methane-saturated medium at HRTs of 16, 8, and 4 h.

from diffusion through the cathode was insignificant during operation and that the vast majority of removal was *via* biotic pathways.

Dissolved methane removal efficiency at a 16 h HRT was high and consistent for reactors A and B,  $84.6 \pm 0.1\%$  and  $83.9 \pm 0.03\%$ , respectively (Fig. 3b). Removal decreased but remained consistent for reactors A and B at an 8 h HRT,  $61.8 \pm 0.1\%$  and  $62.7 \pm 0.1\%$ , respectively. Removal efficiency was higher than in preliminary operation (Fig. 1b) presumably due to adaptation of the microbial community over time. The consistency in dissolved methane removal efficiency but not voltage production at this HRT potentially suggests more instability in *Geobacter* activity between the reactors. Dissolved methane removal efficiency plummeted at a 4 h HRT to  $28.2 \pm 0.1\%$  and  $33.8 \pm 0.04\%$  for reactors A and B, respectively. It is likely that oxygen diffusion into the MFC chamber was too low at such a short HRT to maintain performance given the high dissolved methane loading. According to Cheng *et al.*,<sup>42</sup> oxygen diffusion through the cathode of MFCs is governed by a diffusion coefficient ( $D = 0.000322 \text{ cm}^2 \text{ s}^{-1}$ ), the gradient difference in oxygen concentration outside and inside MFCs ( $7.8 \text{ mg L}^{-1}$ , assumed saturation concentration of oxygen in water), and cathode area ( $A = 60 \text{ cm}^2$ ), resulting in 0.258, 0.129, and  $0.0646 \text{ mg O}_2 \text{ mL}^{-1}$  diffusion for 16, 8, and 4 h HRTs, respectively (ESI† Table S3). Therefore, oxygen availability per influent flow scales linearly with HRT. Dissolved methane removal on a mass/time basis increased as HRT decreased but was relatively similar between 4 and 8 h HRTs (Table 1).

CE and power density for reactors A and B, calculated based on dissolved methane removal efficiency, voltage production, flow rate, and cathode area, decreased as HRT decreased, ranging from 17.7% to 0.888% and  $62.0 \text{ mW m}^{-2}$  to  $2.11 \text{ mW m}^{-2}$ , respectively (Table 1). Low power density was likely attributable to insufficient cathode area ( $60 \text{ cm}^2$ ). Further, the nonoptimal distance between the cathode and the anode may have increased the internal resistance.<sup>51</sup> Therefore, at the longest HRT, a relatively low methane loading ( $1.03 \text{ g d}^{-1}$ ) and high removal efficiency (84.6%) enabled the greatest electrical energy recovery efficiency (17.7%). This CE is similar to those observed in similar single-chamber, air-cathode MFCs operated on other substrates (*e.g.*, glucose or domestic wastewater).<sup>48,52</sup> CE for two-chamber systems,

where oxygen diffusion into the anode chamber is limited, is typically significantly higher than that of single-chamber systems. However, this benefit is offset by energy requirements for aeration in the cathode chamber. It is important to note that CE here is also likely reduced by electrons lost in the initial steps of methanotrophy required to generate metabolites for *Geobacter*.

### 3.3 *Geobacter* and methanotroph activity was spatially distinct in MFCs

*Geobacter* 16S rRNA and *pmoA* transcript copy number were normalized to 16S rRNA copy number to quantify the relative activity of each population at the anode and cathode sites of the bench-scale MFCs. At all HRTs, the relative activity of *Geobacter* in the anode biofilm was approximately  $10^{-1}$  *Geobacter* 16S rRNA copies/total 16S rRNA copies, which was 2 to 3 magnitudes greater than *Geobacter* activity in the cathode biofilm (Fig. 4a). Provided that *Geobacter* rely on the anode to deposit electrons, it is unsurprising that their activity was spatially distributed in this way. Conversely, methanotroph activity profiles indicated significantly greater activity at the cathode relative to the anode in most samples (3 to 4 magnitudes higher; Fig. 4b). Unlike *Geobacter*, methanotrophs can theoretically be active at both the cathode and anode sites; however, their activity is likely highest at the cathode where DO concentrations are high. Recalling our preliminary sequencing data, *Geobacter* relative activity was 41.9% and 6.31% at the reactor A and B anode, respectively, whereas methanotroph relative activity was 4.1% and 5.11% at the reactor A and B anode, respectively, corroborating the spatial distribution of these populations derived from RT-qPCR results. The relative activity of methanotrophs increased as HRT decreased likely due to the increased methane loading, providing additional substrate to methanotrophs. As mentioned above, dissolved methane removal on a mass/time basis increased at lower HRTs, confirming activity data provided *via* RT-qPCR.

It is important to note that the use of 16S rRNA to infer microbial activity has limitations: (1) 16S rRNA copy number does not always perfectly correlate with microbial activity because it includes both growth and non-growth activities, (2) dormant microbes may be present that develop

**Table 1** Average and standard deviation of influent dissolved methane, average methane loading per cathode area, average and standard deviation of methane removal, average methane removal per cathode area, average and standard deviation of voltage production, average power density, and coulombic efficiency at HRTs of 16, 8, and 4 h for reactors A and B

HRT (hours)	Influent dissolved methane ( $\text{mg L}^{-1}$ )	Methane loading per cathode area ( $\text{g d}^{-1} \text{ m}^{-2}$ )	Methane removal (%)	Methane removal per cathode area ( $\text{g d}^{-1} \text{ m}^{-2}$ )	Voltage production (V)	Power density ( $\text{mW m}^{-2}$ )	Coulombic efficiency (%)	
16	Reactor A	$17.1 \pm 1.0$	1.03	$84.6 \pm 0.06$	0.868	$0.610 \pm 0.006$	62.0	17.7
	Reactor B	$17.1 \pm 1.0$	1.03	$83.9 \pm 0.03$	0.861	$0.506 \pm 0.063$	42.7	14.7
8	Reactor A	$17.1 \pm 0.9$	2.05	$61.8 \pm 0.05$	1.27	$0.591 \pm 0.074$	58.2	8.60
	Reactor B	$17.1 \pm 0.9$	2.05	$62.7 \pm 0.07$	1.29	$0.331 \pm 0.080$	18.3	4.81
4	Reactor A	$15.8 \pm 0.5$	3.78	$28.2 \pm 0.05$	1.07	$0.112 \pm 0.037$	2.11	0.888
	Reactor B	$15.0 \pm 0.7$	3.60	$33.8 \pm 0.04$	1.22	$0.301 \pm 0.052$	15.1	2.49

more 16S rRNA to reserve higher protein synthesis potential, and (3) the relationship between 16S rRNA copy number and microbial activity varies among different taxa.<sup>53</sup> Further, normalization of RT-qPCR results to 16S rRNA copy number only provides relative data. Normalizing to biomass extraction weight can circumvent this concern somewhat but requires quantitative RNA extraction which can be challenging given matrix effects that influence extraction efficiency and can vary widely based on biomass source. Alternative approaches such as cell quantification *via* flow cytometry,<sup>54</sup> use of internal standards of marker genes prior to extraction,<sup>55</sup> or other methods could be useful to provide more accurate data regarding microbial activity profiles. The lack of a positive correlation between *Geobacter* and methanotroph activity *via* RT-qPCR as a function of HRT was presumably due to shifts in activity of other microorganisms (*e.g.*, heterotrophic bacteria)

which could have a large impact on activity ratios. It was challenging to normalize RT-qPCR results to biomass extraction weight for anode biofilm samples because anode biofilm biomass was mixed with carbon fibers and difficult to separate. Cathode biofilm biomass was unevenly distributed spatially with varying biofilm thickness apparent from visual observations. Therefore, it was challenging to normalize to cathode area. Despite these methodological limitations, RT-qPCR strongly indicates a distinct spatial activity profile for *Geobacter* and methanotrophs in the methane-driven MFC.

### 3.4 *Geobacter* scavenge methanotrophic metabolites enabling electron recovery from methane

Several studies have reported aerobic methanotrophs excreting intermediate metabolites under oxygen limited conditions (*e.g.*, methanol, formaldehyde, and formate).<sup>23–25,56,57</sup> Methanotrophic intermediate metabolites may also be anaerobically fermented to produce organics such as acetate, lactate, and succinate.<sup>24,25</sup> Based on previous studies,<sup>24,57</sup> aerobic methanotrophs likely yield 50% COD as intermediate metabolites under oxygen limited conditions and use the remaining COD derived from methane for cell synthesis and maintenance activities. Excreted metabolites in the MFCs may then be transported *via* diffusion to *Geobacter* in the anode biofilm. However, metabolites could also be scavenged by heterotrophic bacteria and oxidized to carbon dioxide *via* trace dissolved oxygen unconsumed by methanotrophs. Assuming that formate and acetate are substrates for *Geobacter*, a theoretical energy balance can be derived using bioenergetics (ESI† Table S4). The portion of electrons transferred to the electron acceptor (anode) is thus 0.290 and 0.409 for formate and acetate, respectively. Combined with the observed dissolved methane removal efficiencies at each HRT, approximately 85%, 60%, and 30% at 16 h, 8 h and 4 h, respectively, a theoretical CE of 14.9%, 10.5% and 5.25% for HRTs of 16 h, 8 h, and 4 h, respectively, can be calculated (Fig. 5). This value is comparable to our obtained experimental results (Table 1).

Three likely intermediate metabolites, methanol, formaldehyde, and formate, were added sequentially to the single-chamber MFC with spiked concentrations based on complete conversion of influent dissolved methane to each metabolite on a COD basis (ESI† Table S5). We elected to not add acetate during these experiments as we had previously demonstrated voltage production on acetate during inoculation. Prior to sequential addition of each metabolite, the MFC influent flow was stopped to provide a baseline voltage when no organics were present. After methanol was spiked into the MFC, no significant change in voltage from the baseline was observed (Fig. 6). Then, formaldehyde was injected, resulting in a slight voltage increase (from  $0.0451 \pm 0.0011$  to  $0.0876 \pm 0.0204$ ) lasting for approximately 2 days before voltage decreased to baseline. Finally, formate was added, causing a surge in voltage to 0.546 V which surpassed the peak voltage when previously operated on dissolved methane. Voltage decreased back to baseline after

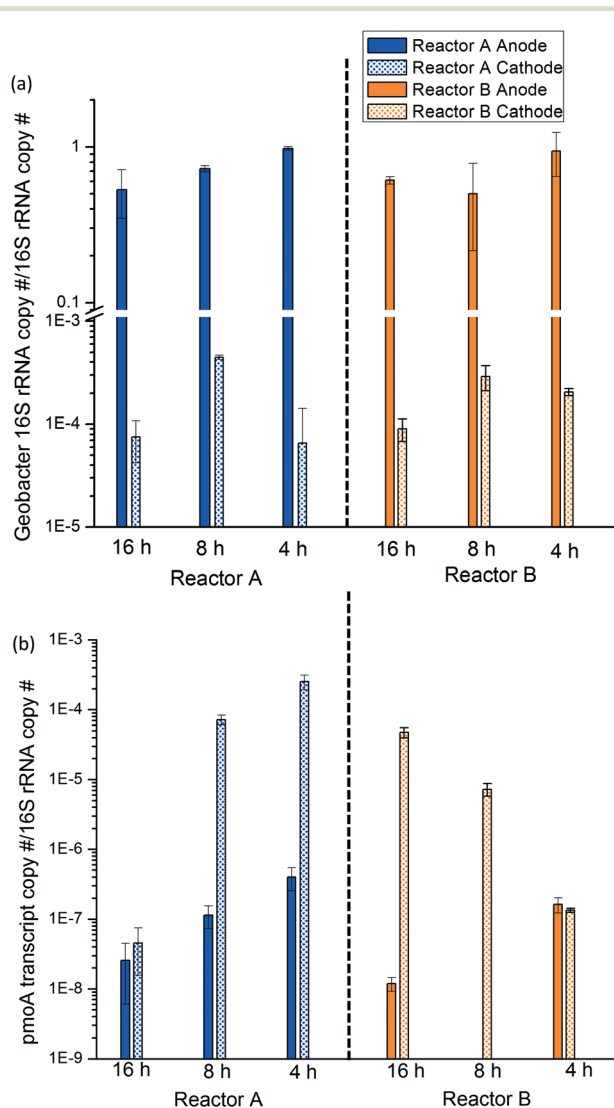


Fig. 4 (a) Relative activity of *geobacter* 16S rRNA gene copy number normalized to total 16S rRNA gene copy number and (b) relative activity of *pmoA* transcript copy number normalized to total 16S rRNA gene copy number in anode and cathode biofilms from reactors A and B at HRTs of 16, 8, and 4 h. Reactor B anode sample not available for *pmoA* at 8 h HRT.

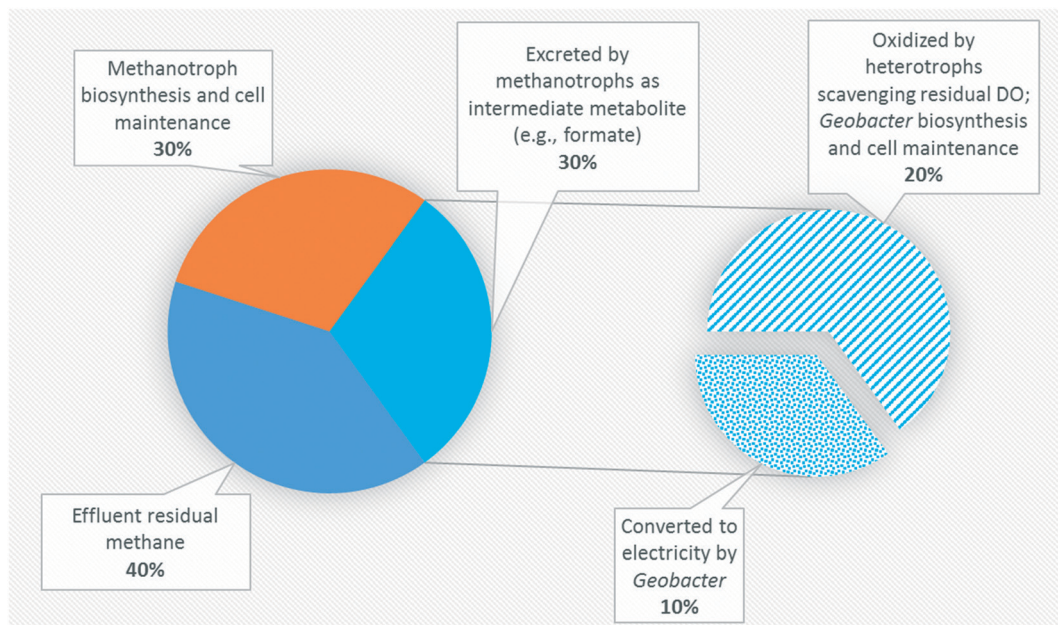


Fig. 5 Theoretical COD balance of dissolved methane removal pathways in an MFC at an HRT of 8 h.

2 days. The CE on formate was 76.1%. Therefore, formate and/or acetate were the likely intermediate metabolites consumed by *Geobacter* in our bench-scale systems. We propose using multiple lines of evidence that air-cathode MFCs can be powered solely on methane *via* a methanotroph-*Geobacter* interaction; methanotrophs in the cathode biofilm oxidize methane to formate which is transported *via* diffusion to the anode biofilm where *Geobacter* converts formate to electrons.

### 3.5 Methane-driven MFCs outcompete existing approaches for dissolved methane management

MFCs are an emerging biotechnology with promise for energy recovery from organic waste streams. Single-chamber, air-cathode MFCs are particularly attractive given that they do not require energy intensive aeration or costly proton exchange membranes. The primary drawback is lower CE due to unavoidable oxygen diffusion into the reactor chamber *via*

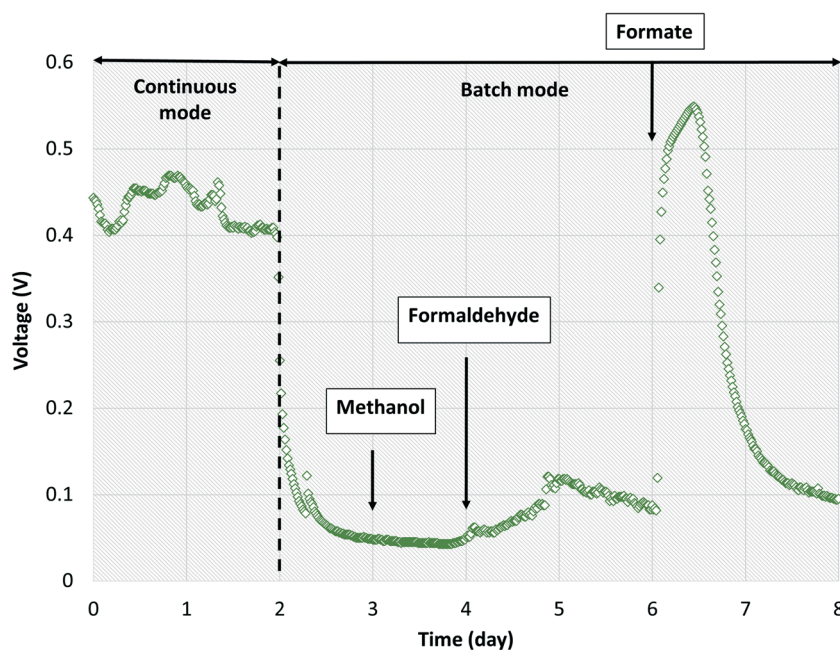


Fig. 6 Voltage production over time with sequential addition of methanol, formaldehyde and formate into single-chamber MFCs operated in batch mode.

**Table 2** Comparison of dissolved methane management approaches including dissolved methane removal, composition of recovered gas, and energy recovery as a percentage based on dissolved methane loading, recovery gas volume, and methane content. An efficiency of 40% was assumed for electricity recovery from collected methane using cogeneration

	System	Operating condition	Dissolved methane removal (%)	Methane content of recovered gas	Energy conversion efficiency (%)
Hatamoto <i>et al.</i> 2010	Down-flow hanging sponge (DHS)	3.8 m <sup>3</sup> air per m <sup>3</sup> , 2 h HRT	95.0	None	N/A
Matsuura <i>et al.</i> 2010	Two-stage DHS	0.25–0.375 m <sup>3</sup> air per m <sup>3</sup> per day first stage, 2.5 m <sup>3</sup> air per m <sup>3</sup> per day second stage	76.8 (single-stage); >99 (dual-stage)	Over 30% methane in the recovered gas	12.0
Cookney <i>et al.</i> 2012	Sweep gas membrane contactor	Lowest liquid velocity 0.0033 m s <sup>-1</sup> , coupled with 0.85 L min <sup>-1</sup> gas flow	72.0	0.028 vol% in the recovered gas	N/A
Cookney <i>et al.</i> 2016	Sweep gas membrane contactor	Sweep gas to liquid flow ratio 0.034	98.0	53.0%	21.2
Bandara <i>et al.</i> 2011	Vacuum degassing membrane module	Vacuum maintained at 50 kPa	68.0 ± 7.0	22.0 ± 13.0%	8.80

the cathode and issues with scalability as reviewed in ref. 51. Despite these limitations, MFCs may be attractive to manage dissolved methane in anaerobic effluents or to power sensors in marine applications (*i.e.*, benthic microbial fuel cells<sup>34</sup>). Current approaches for dissolved methane management in anaerobic effluents are either energy intensive or fail to recover energy because they oxidize dissolved methane to carbon dioxide or recover a gas of insufficient methane content for energy recovery *via* cogeneration. Matsuura *et al.*<sup>7</sup> recovered 30% of influent dissolved methane using a two-stage down-flow hanging sponge system. Bandara *et al.*<sup>9</sup> achieved 22 ± 13% methane recovery using a vacuum degassing membrane module. Cookney *et al.*<sup>8</sup> had the highest methane recovery, 53%, *via* a sweep gas membrane contactor. However, these approaches have high energy demands due to relatively high air/liquid ratio requirements for hanging sponge systems and a high vacuum pressure requirement for degassing membranes. Moreover, dissolved methane that is stripped out of liquid is diluted with air in the hanging sponge system, making the collected gas mixture non-reusable for energy recovery. With degassing membranes, coexisting dissolved gases such as nitrogen and carbon dioxide are also recovered significantly diluting methane in the off-gas.<sup>10</sup> Subsequent purification of recovered gas would further increase energy requirements and costs of dissolved methane energy recovery.<sup>58</sup> Considering that methane conversion efficiency to electricity *via* cogeneration is relatively low, less than 40%, electricity recovery from dissolved methane in the aforementioned studies was at most 12.0%, 8.80%, and 21.2%, respectively. Therefore, little energy was recovered and significant GHG emissions remain a concern. Further, this does not consider energy demands for these systems which likely exceed energy recovery. Although our experimental work indicated a rather low maximum of 17.7% conversion of dissolved methane to electricity, removal was significantly greater than those of previous studies (up to 85%; Table 2) resulting in a more substantial decrease in GHG emissions. Therefore, MFCs generally outperform existing technologies when considering both energy recovery and GHG emissions.

## 4. Conclusions

Bench-scale MFCs treating a synthetic anaerobic effluent demonstrated up to 85% dissolved methane removal, 0.5 to 0.6 V generation, and a maximum CE of 17.7%. High-throughput sequencing of anode biofilm samples indicated a high activity of *Geobacter* and methanotrophs, substantiating voltage production and suggesting a methanotroph–exoelectrogen interaction, with formate/acetate the likely intermediate metabolites. RT-qPCR results suggested that methane oxidation and *Geobacter* extracellular electron transfer occurred primarily at the cathode biofilm and anode biofilm, respectively. Therefore, oxygen diffusion and HRT (inter-connected parameters) were correlated with methane removal efficiency and voltage production, indicating that longer HRTs improve methane removal due to additional oxygen availability for methanotrophs. Future research using advanced methods (*e.g.*, <sup>13</sup>C labeled methane using RNA-stable isotopic probing or fluorescent *in situ* hybridization targeting methanotrophs and *Geobacter*) are necessary to elucidate the methanotroph–exoelectrogen interaction suggested here in a methane-driven MFC. This study demonstrated that MFCs are able to be solely powered by dissolved methane, which presents MFCs as a potentially promising technology for post-treatment of anaerobic effluents.

## Conflicts of interest

There are no conflicts to declare.

## Acknowledgements

Siming Chen is partially funded by the China Scholarship Council. The authors wish to thank Caroline Kim for her laboratory assistance. The authors would also like to thank Dipak Patel for help with sampling at the Hyperion Wastewater Treatment Plant.

## References

- 1 A. Smith, S. Skerlos and L. Raskin, Anaerobic membrane bioreactor treatment of domestic wastewater at psychrophilic temperatures ranging from 15 C to 3 C, *Environ. Sci.: Water Res. Technol.*, 2015, 1(1), 56–64.
- 2 R. Yoo, *et al.*, Effect of temperature on the treatment of domestic wastewater with a staged anaerobic fluidized membrane bioreactor, *Water Sci. Technol.*, 2014, 69(6), 1145–1150.
- 3 A. L. Smith, S. J. Skerlos and L. Raskin, Membrane biofilm development improves COD removal in anaerobic membrane bioreactor wastewater treatment, *Microb. Biotechnol.*, 2015, 8(5), 883–894.
- 4 A. L. Smith, *et al.*, Navigating wastewater energy recovery strategies: a life cycle comparison of anaerobic membrane bioreactor and conventional treatment systems with anaerobic digestion, *Environ. Sci. Technol.*, 2014, 48(10), 5972–5981.
- 5 A. L. Smith, S. J. Skerlos and L. Raskin, Psychrophilic anaerobic membrane bioreactor treatment of domestic wastewater, *Water Res.*, 2013, 47(4), 1655–1665.
- 6 J. Giménez, *et al.*, Methane recovery efficiency in a submerged anaerobic membrane bioreactor (SAnMBR) treating sulphate-rich urban wastewater: evaluation of methane losses with the effluent, *Bioresour. Technol.*, 2012, 118, 67–72.
- 7 N. Matsuura, *et al.*, Closed DHS system to prevent dissolved methane emissions as greenhouse gas in anaerobic wastewater treatment by its recovery and biological oxidation, *Water Sci. Technol.*, 2010, 61(9), 2407–2415.
- 8 J. Cookney, *et al.*, Dissolved methane recovery from anaerobic effluents using hollow fibre membrane contactors, *J. Membr. Sci.*, 2016, 502, 141–150.
- 9 W. M. Bandara, *et al.*, Removal of residual dissolved methane gas in an upflow anaerobic sludge blanket reactor treating low-strength wastewater at low temperature with degassing membrane, *Water Res.*, 2011, 45(11), 3533–3540.
- 10 M. Henares, *et al.*, Comparative study of degassing membrane modules for the removal of methane from Expanded Granular Sludge Bed anaerobic reactor effluent, *Sep. Purif. Technol.*, 2016, 170, 22–29.
- 11 G. Luo, W. Wang and I. Angelidaki, A new degassing membrane coupled upflow anaerobic sludge blanket (UASB) reactor to achieve in-situ biogas upgrading and recovery of dissolved CH<sub>4</sub> from the anaerobic effluent, *Appl. Energy*, 2014, 132, 536–542.
- 12 A. McLeod, B. Jefferson and E. J. McAdam, Toward gas-phase controlled mass transfer in micro-porous membrane contactors for recovery and concentration of dissolved methane in the gas phase, *J. Membr. Sci.*, 2016, 510, 466–471.
- 13 J. Cookney, *et al.*, Recovery of methane from anaerobic process effluent using poly-di-methyl-siloxane membrane contactors, *Water Sci. Technol.*, 2012, 65(4), 604–610.
- 14 N. Iversen and B. Jørgensen, Anaerobic methane oxidation rates at the sulfate-methane transition in marine sediments from Kattegat and Skagerrak (Denmark), *Limnol. Oceanogr.*, 1985, 30(5), 944–955.
- 15 A. Boetius, *et al.*, A marine microbial consortium apparently mediating anaerobic oxidation of methane, *Nature*, 2000, 407(6804), 623–626.
- 16 S. Islas-Lima, F. Thalasso and J. Gomez-Hernandez, Evidence of anoxic methane oxidation coupled to denitrification, *Water Res.*, 2004, 38(1), 13–16.
- 17 A. A. Raghoebarsing, *et al.*, A microbial consortium couples anaerobic methane oxidation to denitrification, *Nature*, 2006, 440(7086), 918–921.
- 18 K. Knittel and A. Boetius, Anaerobic oxidation of methane: progress with an unknown process, *Annu. Rev. Microbiol.*, 2009, 63, 311–334.
- 19 J. Delgado Vela, *et al.*, Prospects for biological nitrogen removal from anaerobic effluents during mainstream wastewater treatment, *Environ. Sci. Technol. Lett.*, 2015, 2(9), 234–244.
- 20 R. S. Hanson and T. E. Hanson, Methanotrophic bacteria, *Microbiol. Rev.*, 1996, 60(2), 439–471.
- 21 M. G. Kalyuzhnaya, A. W. Puri and M. E. Lidstrom, Metabolic engineering in methanotrophic bacteria, *Metab. Eng.*, 2015, 29, 142–152.
- 22 P. J. Strong, S. Xie and W. P. Clarke, Methane as a resource: can the methanotrophs add value?, *Environ. Sci. Technol.*, 2015, 49(7), 4001–4018.
- 23 Y. Morinaga, *et al.*, Methane metabolism of the obligate methane-utilizing bacterium, *Methylomonas flagellata*, in methane-limited and oxygen-limited chemostat culture, *Agric. Biol. Chem.*, 1979, 43(12), 2453–2458.
- 24 M. G. Kalyuzhnaya, *et al.*, Highly efficient methane biocatalysis revealed in a methanotrophic bacterium, *Nat. Commun.*, 2013, 4, 2785.
- 25 A. Gilman, *et al.*, Bioreactor performance parameters for an industrially-promising methanotroph *Methylomicrobium buryatense* 5GB1, *Microb. Cell Fact.*, 2015, 14(1), 182.
- 26 P. J. Strong, *et al.*, The opportunity for high-performance biomaterials from methane, *Microorganisms*, 2016, 4(1), 11.
- 27 B. E. Logan, *et al.*, Microbial fuel cells: methodology and technology, *Environ. Sci. Technol.*, 2006, 40(17), 5181–5192.
- 28 K. Rabaey and W. Verstraete, Microbial fuel cells: novel biotechnology for energy generation, *Trends Biotechnol.*, 2005, 23(6), 291–298.
- 29 K. Rabaey, *et al.*, Microbial fuel cells for sulfide removal, *Environ. Sci. Technol.*, 2006, 40(17), 5218–5224.
- 30 W.-W. Li, H.-Q. Yu and Z. He, Towards sustainable wastewater treatment by using microbial fuel cells-centered technologies, *Energy Environ. Sci.*, 2014, 7(3), 911–924.
- 31 L. Ren, Y. Ahn and B. E. Logan, A two-stage microbial fuel cell and anaerobic fluidized bed membrane bioreactor (MFC-AFMBR) system for effective domestic wastewater treatment, *Environ. Sci. Technol.*, 2014, 48(7), 4199–4206.
- 32 Y. Tian, *et al.*, In-situ integration of microbial fuel cell with hollow-fiber membrane bioreactor for wastewater treatment

- and membrane fouling mitigation, *Biosens. Bioelectron.*, 2015, **64**, 189–195.
- 33 K.-Y. Kim, *et al.*, Performance of anaerobic fluidized membrane bioreactors using effluents of microbial fuel cells treating domestic wastewater, *Bioresour. Technol.*, 2016, **208**, 58–63.
- 34 C. Donovan, *et al.*, Batteryless, wireless sensor powered by a sediment microbial fuel cell, *Environ. Sci. Technol.*, 2008, **42**(22), 8591–8596.
- 35 P. Girguis and C. E. Reimers, Methane-powered microbial fuel cells, *US Pat.*, Application No. 12/994,598, 2011.
- 36 Z. J. Ren, Running on gas, *Nature*, 2017, **2**(17093), 1.
- 37 W. van Hees, A bacterial methane fuel cell, *J. Electrochem. Soc.*, 1965, **112**(3), 258–262.
- 38 J. Ding, *et al.*, Decoupling of DAMO archaea from DAMO bacteria in a methane-driven microbial fuel cell, *Water Res.*, 2017, **110**, 112–119.
- 39 M. J. McNulty, V. G. Poosarla, K.-Y. Kim, R. Jasso-Chávez, B. E. Logan and T. K. Wood, Electricity from methane by reversing methanogenesis, *Nat. Commun.*, 2017, **8**, 15419.
- 40 Y. Ahn and B. E. Logan, A multi-electrode continuous flow microbial fuel cell with separator electrode assembly design, *Appl. Microbiol. Biotechnol.*, 2012, **93**(5), 2241–2248.
- 41 Y. Feng, *et al.*, Treatment of carbon fiber brush anodes for improving power generation in air-cathode microbial fuel cells, *J. Power Sources*, 2010, **195**(7), 1841–1844.
- 42 S. Cheng, H. Liu and B. E. Logan, Increased performance of single-chamber microbial fuel cells using an improved cathode structure, *Electrochem. Commun.*, 2006, **8**(3), 489–494.
- 43 J. J. Kozich, *et al.*, Development of a dual-index sequencing strategy and curation pipeline for analyzing amplicon sequence data on the MiSeq Illumina sequencing platform, *Appl. Environ. Microbiol.*, 2013, **79**(17), 5112–5120.
- 44 P. D. Schloss, *et al.*, Introducing mothur: open-source, platform-independent, community-supported software for describing and comparing microbial communities, *Appl. Environ. Microbiol.*, 2009, **75**(23), 7537–7541.
- 45 E. Pruesse, *et al.*, SILVA: a comprehensive online resource for quality checked and aligned ribosomal RNA sequence data compatible with ARB, *Nucleic Acids Res.*, 2007, **35**(21), 7188–7196.
- 46 D. E. Cummings, *et al.*, Diversity of Geobacteraceae species inhabiting metal-polluted freshwater lake sediments ascertained by 16S rDNA analyses, *Microb. Ecol.*, 2003, **46**(2), 257–269.
- 47 D. G. Bourne, I. R. McDonald and J. C. Murrell, Comparison of pmoA PCR primer sets as tools for investigating methanotroph diversity in three Danish soils, *Appl. Environ. Microbiol.*, 2001, **67**(9), 3802–3809.
- 48 H. Liu and B. E. Logan, Electricity generation using an air-cathode single chamber microbial fuel cell in the presence and absence of a proton exchange membrane, *Environ. Sci. Technol.*, 2004, **38**(14), 4040–4046.
- 49 D. Xing, *et al.*, Electricity generation by *Rhodospseudomonas palustris* DX-1, *Environ. Sci. Technol.*, 2008, **42**(11), 4146–4151.
- 50 R. Whittenbury, K. Phillips and J. Wilkinson, Enrichment, isolation and some properties of methane-utilizing bacteria, *Microbiology*, 1970, **61**(2), 205–218.
- 51 B. E. Logan, *et al.*, Assessment of microbial fuel cell configurations and power densities, *Environ. Sci. Technol. Lett.*, 2015, 206–214.
- 52 P. Aelterman, *et al.*, Continuous electricity generation at high voltages and currents using stacked microbial fuel cells, *Environ. Sci. Technol.*, 2006, **40**(10), 3388–3394.
- 53 S. J. Blazewicz, *et al.*, Evaluating rRNA as an indicator of microbial activity in environmental communities: limitations and uses, *ISME J.*, 2013, **7**(11), 2061–2068.
- 54 R. Props, *et al.*, Absolute quantification of microbial taxon abundances, *ISME J.*, 2016, **11**, 584–587.
- 55 W. Smets, *et al.*, A method for simultaneous measurement of soil bacterial abundances and community composition via 16S rRNA gene sequencing, *Soil Biol. Biochem.*, 2016, **96**, 145–151.
- 56 B. T. Eshinimaev, *et al.*, Physiological, biochemical, and cytological characteristics of a haloalkalitolerant methanotroph grown on methanol, *Microbiology*, 2002, **71**(5), 512–518.
- 57 G.-Y. Rhee and G. W. Fuhs, Wastewater denitrification with one-carbon compounds as energy source, *J. - Water Pollut. Control Fed.*, 1978, 2111–2119.
- 58 C. Vallieres and E. Favre, Vacuum versus sweeping gas operation for binary mixtures separation by dense membrane processes, *J. Membr. Sci.*, 2004, **244**(1), 17–23.